Catastrophic SEE in High-Voltage Power MOSFETs

L. E. Selva, L. Z. Scheick, S. McClure, T. Miyahira, S. M. Guertin, S. K. Shah, L. D. Edmonds and J. D. Patterson

Abstract—Heavy ion irradiation of high-voltage power MOSFETs with long-range ions (>123µm in silicon) was performed using 14, 19, 22, 24, 28, and 39 MeV-cm^2/mg ions at normal incidence. Prior to catastrophic failure some DUTs exhibited unusual electrical characteristic: all devices demonstrated high current transients (or current spikes) at voltages significantly lower than the voltage at which the devices failed.

I. INTRODUCTION

High-voltage power MOSFETs have not been widely used in past space missions. However, there is a current and increasing interest within NASA for utilizing them in future missions. For example, as laser drivers for near Earth orbits and as power switches in orbiters about the Jovian system. Radiation testing and evaluation of MOSFETs with high-voltage rating (500V or greater) present new technical challenge, which test engineers must address. There is little

L. E. Selva is with Jet Propulsion Laboratory-California Institute of Technology, Pasadena, CA 91109-8099, USA (telephone: 818-354-5751, email: luis.e.selva@jpl.nasa.gov) and UCLA School of Medicine, Department of Biomedical Physics.

L. Z. Scheick is with Jet Propulsion Laboratory-California Institute of Technology, Pasadena, CA 91109-8099, USA (telephone: 818-354-3272, email: leif.z.scheick@jpl.nasa.gov).

S. McClure is with Jet Propulsion Laboratory-California Institute of Technology, Pasadena, CA 91109-8099, USA (telephone: 818-354-0484, email: s.mcclure@jpl.nasa.gov).

T. F. Miyahira is with Jet Propulsion Laboratory-California Institute of Technology, Pasadena, CA 91109-8099, USA (telephone: 818-354-2908, email: tetsuo.f.miyahira@jpl.nasa.gov).

S. M. Guertin is with Jet Propulsion Laboratory-California Institute of Technology, Pasadena, CA 91109-8099, USA (telephone: 818-354-1637, email: steven.m.guertin@jpl.nasa.gov).

S. K. Shah is with Jet Propulsion Laboratory-California Institute of Technology, Pasadena, CA 91109-8099, USA (telephone: 818-354-5751, email: sumit.k.shah@jpl.nasa.gov) and UCLA School of Medicine, Department of Biomedical Physics.

L. D. Edmonds is with Jet Propulsion Laboratory-California Institute of Technology, Pasadena, CA 91109-8099, USA (telephone: 818-354-2778, email: larry.d.edmonds@jpl.nasa.gov).

J. D. Patterson is with Jet Propulsion Laboratory-California Institute of Technology, Pasadena, CA 91109-8099, USA (telephone: 818-393-6872, email: jeffrey.d.patterson@jpl.nasa.gov).

information (specifically, range adequacy issues) available in the literature regarding the performance of high-voltage power MOSFETs in radiation environments. In this paper, SEGR and SEB results from a variety of high-voltage power MOSFETs (550V to 1000V) manufactured by Fairchild, Advance Power Technology, and International Rectifier are presented.

II. DEVICE DESCRIPTION

All of the power MOSFETs tested were N-channel enhancement mode with gate-to-source (V_{GS}) voltage rating of ± 20 volts with the exception of the Advance Power Technology devices which have a voltage rating of ± 30 volts. Table I lists key properties of the MOSFETs used in this experiment. Epitaxial depth and doping levels were determined by spreading resistance measurements, which were conducted by Solecon Laboratories Incorporated using the four-point probe measurement technique.

TABLE I: MANUFACTURER INFORMATION FOR THE POWER MOSFETs USED IN THIS EXPERIMENT.

Part #	Manu-facturer	Date code	Depth (µm)	Doping (ions/cm^3)
IRHY7G30 CMSE	IR	0048	100	~1x10^{14}
			113	~1x10^{14}
IRFMG40	IR	9366*	100	~1x10^{14}
IRHY7434 CSE (550V)	IR	Un-known	Un-known	Un-Known
RFP4N100	Fair-child	Un-known	125	~1x10^{14}
APT10088 HVR	APT	0218	Un-known	Un-Known
APT1004R CN	APT	0042	100	~1x10^{14}

*Split into two groups: flight and non-flight.

Of the six power MOSFET types used in this experiment only two were radiation hardened, i.e., IRHY7G30CMSE and

the IRHY7434CSE. These devices have a V_{DS} rating of 1000V and 550V, respectively.

The IRHY7G30CMSE device came from the date code 0048 and wafer lot B9003. Two engineering samples from the IRHY7G30CMSE were also tested. The engineering samples I and II were from different design development phases, which may have included variations in guard rings, doping concentrations and epitaxial depth. Specific details were not made available to the authors.

The IRHY7434CSE was an unscreened Bosch 550V power MOSFET packaged in a TO-254 configuration.

The IRFMG40 test group was split into two groups, flight and non-flight. The flight group was designated as such based on the additional screening performed on them by the manufacturer. The non-flight group was unscreened.

Two MOSFETs by Advance Power Technology were tested, the APT1004RCN and the APT10088HVR. Both device types are rated at 1000V and are packaged in a TO-257 configuration. The only visible difference between these two devices is the die area, which is four times greater for the APT10088HVR than for the APT1004RCN.

The Fairchild RFP4N100 was also tested. This device came on a plastic TO-220 package. The date code was 0042.

III. EXPERIMENTAL DETAILS

A. Single Event Failure Criteria

SEGR and SEB are two types of catastrophic events that destroy the functionality of a power MOSFET [1-6]. SEGR destroys the ability of the gate to regulate the current flow from the source to the drain by permanently damaging the gate insulator (SiO_2). SEB, on the other hand, does not damage the insulator but effectively shorts the source to the drain. SEGR and SEB were defined as points on the V_{DS}, V_{GS} plane where the off current (gate, drain, or source) exceeded 1µA during or following irradiation. The drain-to-source voltage (V_{DS}) at which the device failed was termed the critical voltage and is the value that is plotted. These figures will be discussed in a latter section of this paper.

B. Electrical Stress Measurements

Non-destructive electrical breakdown measurements were made on all MOSFETs prior to irradiation using a Tektronix curve tracer type 576. The average and standard deviation of breakdown (V_{DS}) for each device type was determined and is listed on Table II. The curve tracer was current limited to 10µA.

TABLE II: NON-DESTRUCTIVE ELECTRICAL BREAKDOWN RESULTS.

Part Number	Ave. Breakdown (volts)	Standard Deviation (volts)	Sample Size
IRFMG40 (non-flight)	1124.44	± 6.16	18
IRFMG40 (flight)	1132.35	± 23.86	19
IRHY7G30CMSE	1310.00	± 89.44	16
Engineering sample I	1217.50	± 180.07	10
Engineering sample II	1021.25	± 44.54	11
IRHY7434CSE	615.26	± 25.25	19
RFP4N100	1099.29	± 60.85	28
APT1004RCN	1119.00	± 15.95	10
APT10088HVR	1109.60	± 19.89	25

C. Ion Selection

All test devices were irradiated at the Texas A&M Cyclotron with long-range ions. The krypton and xenon ions were selected for their ability to penetrate and exit the epitaxial region of each power MOSFET. Multiple values of Linear Energy Transfer (LET) for krypton (^{78}Kr) were obtained by using degrader. Xenon (^{129}Xe) ions with LET of 39.6 MeV-cm^2/mg were also used in this experiment. Table III lists the ions used in this experiment along with ions used by International Rectifier, which were tested at Brookhaven National Laboratory (BNL) TVDG [7].

TABLE III: LIST OF IONS USED.

Ion	Energy (MeV)	Range in Silicon (µm)	Incident LET(MeV-cm^2/mg)
^{78}Kr	3120	601	14.2
^{78}Kr	2098*	320	19.0
^{78}Kr	1656*	243	22.0
^{78}Kr	1342*	185	24.6
^{78}Kr	948*	123	28.0
^{129}Xe	3197	254	39.6
^{79}Br	305**	33	39.8
^{127}I	343**	39	60.0

*Beam energy degraded by using degrader.
**Beam used by IR to test IRHY7G30CMSE at BNL.

D. Biasing Conditions

Biasing conditions during irradiation was performed in any one of two gate-to-source (V_{GS}) voltages, i.e., –2V or –10V. A –20V gate-to-source was utilized to characterize the IRFMG40 non-flight group. The drain-to-source voltage (V_{DS}) was incremented in steps of 25 volts until SEGR or/and SEB occurred. No stiffening capacitors or current limiting resistors were placed between device and the power supply. At each voltage step, the DUT was irradiated with a minimum fluence of 5×10^5 particles/cm^2 and a flux of about 4×10^4 particles/cm^2 per second.

Prior to and following each irradiation, the DUT was measured with V_{GS} = specification maximum (–20V or –30V) and V_{DS} = 0 volts followed by V_{DS} = specification maximum (1000V) and V_{GS} = 0 volts. If the DUT was still operational, the voltage was stepped up and the device was irradiated again. All DUTs were biased and measured with a Hewlett-Packard HP4142B high voltage module (current limited to 1mA) connected to a personal computer (PC) via a general purpose instrument bus (GPIB).
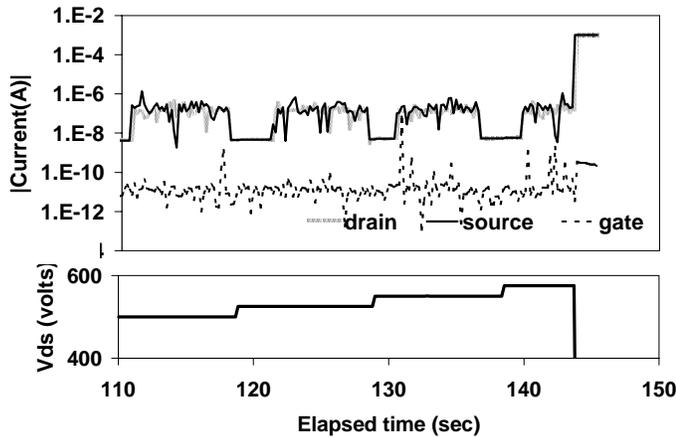
IV. TEST RESULTS

A. In Situ Measurements

Figure 1: In situ DUT measurements for the IRHY7434CSE using ^{78}Kr ions with LET of 19.2MeV-cm^2/mg (V_{GS} = -2V).

Figure 1 is a strip chart of an IRHY7434CSE power MOSFET that failed due to SEB. The primary y-axis is the in situ current measurements taken a fraction of a second prior to and following each irradiation. During irradiation, the gate, source, and drain current was sampled ~3 times per second. The secondary y-axis is the drain-to-source voltage supplied to the DUT during the experiment. The x-axis presents the elapsed time in seconds.

Prior to the start of each irradiation, the DUT drew ~5×10^{-9} A at both the drain and the source and about 1×10^{-11} A at the gate. During the irradiation, the drain and source currents increased by 2 orders of magnitude which lasted for the entire period of irradiation (~10 seconds). At failure, the current was

1mA, which is the current limit. The in situ measurements for the gate and source currents during irradiation show current spikes that lasted equal to or less than the sampling period. The transient current (or current spikes) ranged from 0 to 4 orders of magnitude. At the point of failure, the gate current was ~1×10^{-11} A. As can be inferred from Figure 1, the insulator (SiO$_2$) layer was not damaged by any of the current transients that were generated at the oxide or at the epitaxial layer. SEB occurred at a V_{DS} of 575 volts (close to the electrical breakdown value of 615.26 ± 25.25 volts).
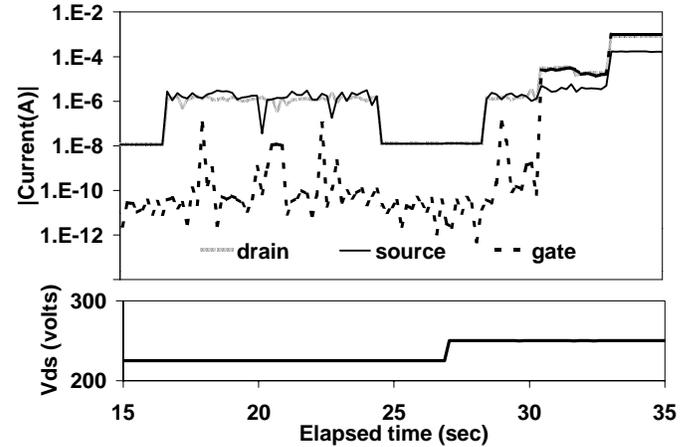

Figure 2: In situ DUT measurements for the APT10088 using ^{78}Kr ion with LET of 19.2MeV-cm^2/mg (V_{GS} = -10V).

Figure 2 shows a strip chart for an Advance Power Technology (APT10088HVR) power MOSFET that was irradiated with ^{78}Kr ions. Prior to and following irradiation steps, the gate current was ~1×10^{-12} A. During irradiation, the strip chart recorded current transients that lasted longer than the sampling period. The SiO$_2$ layer ruptured at a V_{DS} of 250 volts, well below the electrical breakdown measurement of 1109.60 ± 19.89 volts.
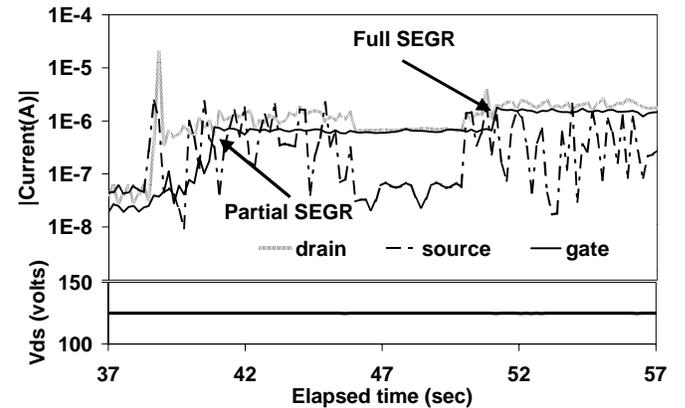

Figure 3: In situ DUT measurement for the RFP4N100 using ^{129}Xe ions with LET of 39.6MeV-cm^2/mg (V_{GS} = -2V).

Figure 3 shows a 20 second strip chart of an RFP4N100 power MOSFET that was irradiated with ^{129}Xe ions. The DUT failed due to gate rupture at a V_{DS} of 125 volts. Gate current prior to irradiation was ~1×10^{-8} A and at the point of failure, the current was ~6×10^{-7} A, which according to the failure criterion is not a "full" gate rupture and therefore was classified as a partial gate rupture. At the 46th second of the in situ measurement, the beam went down for 5 seconds before resuming the irradiation. Upon resuming, the gate was furthered damaged and the current increased to over 1μA.
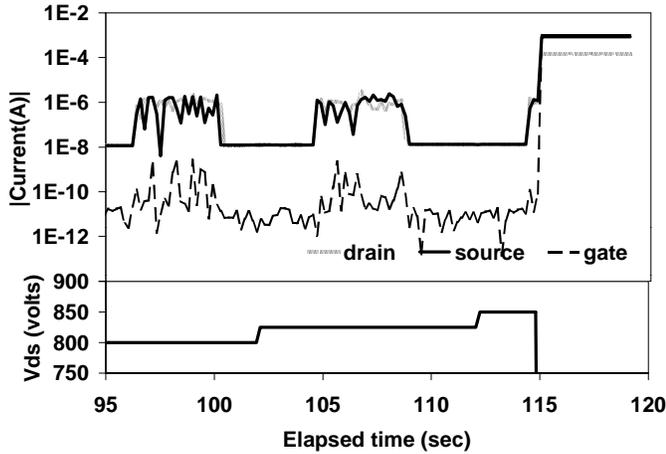

Figure 4: In situ DUT measurements for the IRYH7G30 Engineering Sample II using ^{78}Kr ions with LET of 24.6MeV-cm^2/mg.

Figure 4 shows a strip chart for an IRHY7G30CMSE (Engineering Sample II) that was irradiated with ^{78}Kr ions. The failure mode of this DUT was SEGR. However, the dominant current flow was from gate to source not from gate to drain, as observed in figures 2 and 3. Gate rupture occurred at the 115th second, where the gate current increased to 1mA (current limit) and V_{DS} dropped from 850 to zero volts.
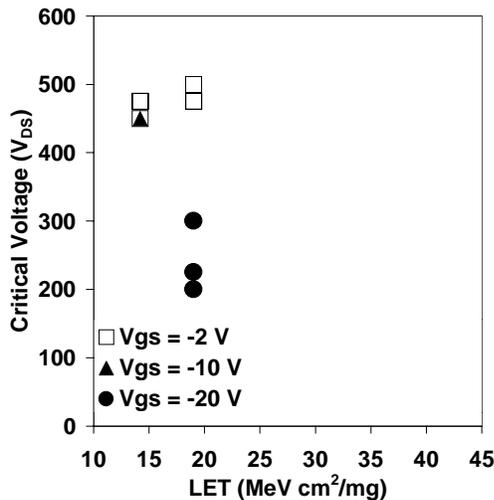
B. Radiation Response

Figure 5: Radiation response of the IRFMG40 (non-flight lot).

Figures 5 through 12 show the radiation response of the various MOSFET types used in this experiment and are plotted as critical voltage versus incident LET. Instead of error bars in each figure, all the data are plotted in order to highlight the failure variability for a given LET and bias condition.
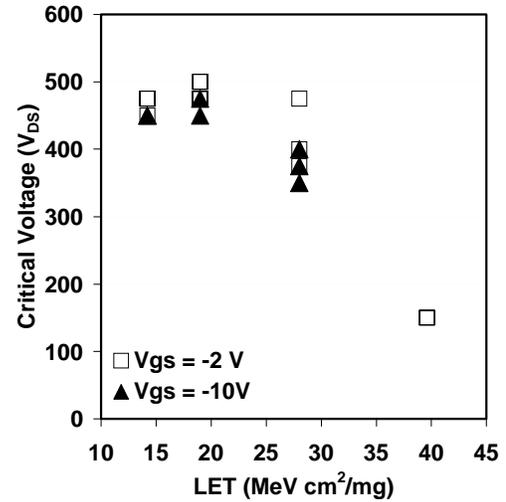

Figure 6: Radiation response of the IRFMG40 (flight lot).

Figure 5 and 6 represents the radiation response of the IRFMG40 non-flight lot and fight lot, respectively. The non-flight lot was biased at –2, –10and –20 volts (V_{GS}). The flight lot was biased at –2 and –10 volts. All failures were due to gate rupture. At relatively low LET (14 and 19 MeV-cm^2/mg) both groups failed well below the electrical breakdown values (by ~ 40%), as shown in Table II. At an LET of 39.6MeV-cm^2/mg, the flight group DUT failed at a V_{DS} of 125V with a V_{GS} of –2V.
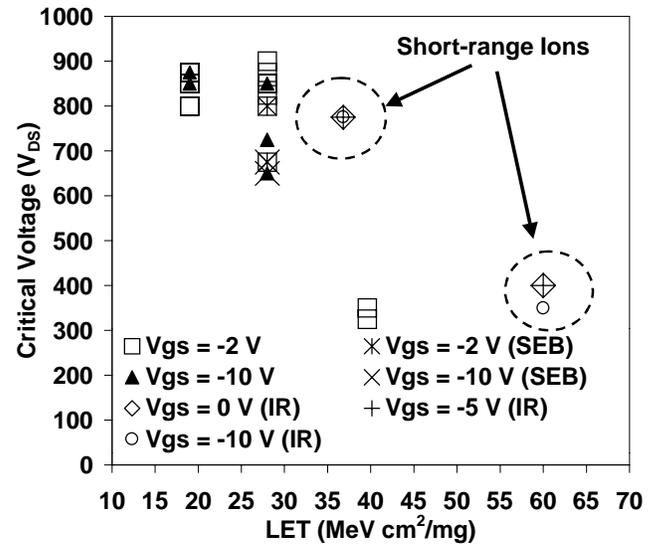

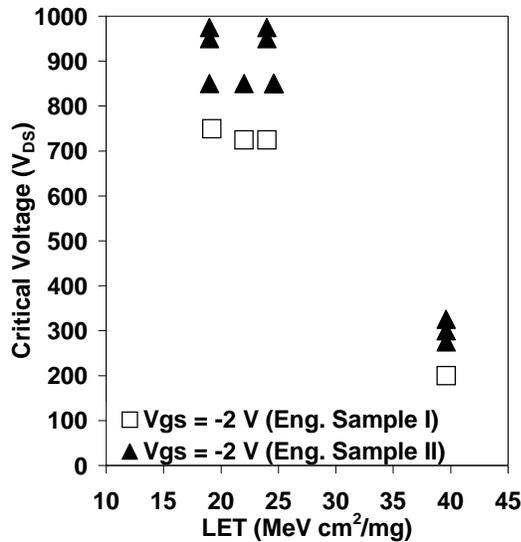Figure 7: Radiation response of the IRHY7G30CMSE.

Figure 8: Radiation response of the IRHY7G30CMSE (Engineering samples I and II).

Figures 7 and 8 represent the radiation response of the IRHY7G30CMSE, and engineering samples I and II, respectively. Figure 7 is a composite of two data sets, one is from the data set that was acquired with long-range ions and the other is from the radiation experiment(s) reported by the manufacturer. Table III lists the ions that the manufacturer used. The two large dashed circles show the manufacture's data [7]. The two data sets overlap at an LET of 39 MeV-cm^2/mg. At this same LET value regardless of the bias conditions (0V, -5V, -10V), the short-range ions did not elicit a failure until a V_{DS} of 775V. However, when long-range ions were used with the same LET, failure was induced at a V_{DS} of 300V. In figure 7, failure points are labeled by a V_{GS} voltage followed by nothing or (SEB) or (IR), which represent SEGR failure, SEB failure or International Rectifier data with an unknown type of failure (SEGR or SEB). At low LET values (14, 19 and 22 MeV-cm^2/mg) all three MOSFET groups failed below the electrical breakdown values by 70%, 62% and 83%, respectively; corresponding derated values (relative to 1000V) are 90%, 75% and 85%, respectively. Based on these test results IR has modified and upgraded the IRHY7G30CMSE product. Note that short-range ions overestimate the onset of V_{DS} for SEGR by as much as 400V.

Figure 9 and 10 represent the radiation response of the APT1004RCN and APT10088HVR by Advance Power Technology. At low LET values both device types failed below their expected electrical breakdown values by 45% and 43% at the highest failure, respectively. In Figure 10, the spread in failure for the gate-to-source bias of –10 volts, suggests part-to-part variation that may effect the applied electric field across the insulator (SiO_2). The part-to-part variation may be due slight variation in SiO_2 thicknesses or from slight differences in epitaxial doping.

Figure 11 shows the radiation response of the RFP4N100 power MOSFET by Fairchild. At low LET values the device failed below the expected electrical breakdown value by 52%.

Figure 12 shows the radiation response of the IRHY7434. The radiation harden IRHY7434 was the only 550V power MOSFET that was tested. At low LET values, the device failed above the rated voltage of 550V, but less than the expected electrical breakdown value of 615.25 ± 25.25 volts.
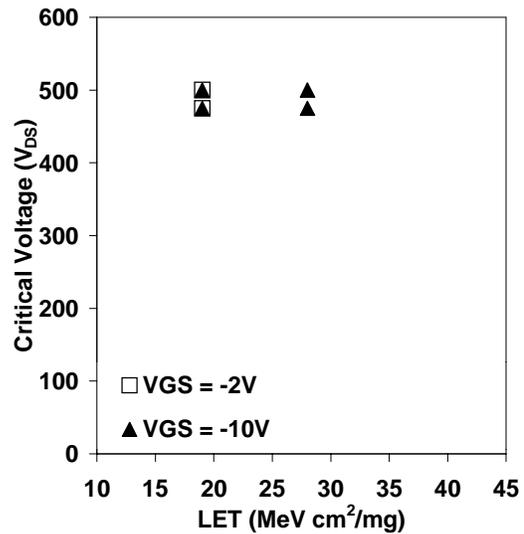

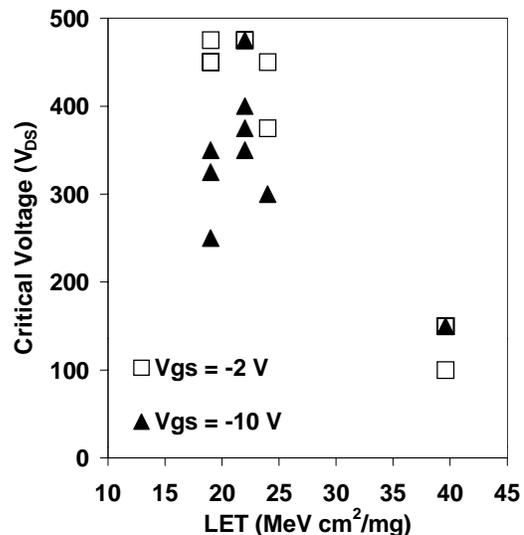Figure 9: Radiation response of APT1004RCN.

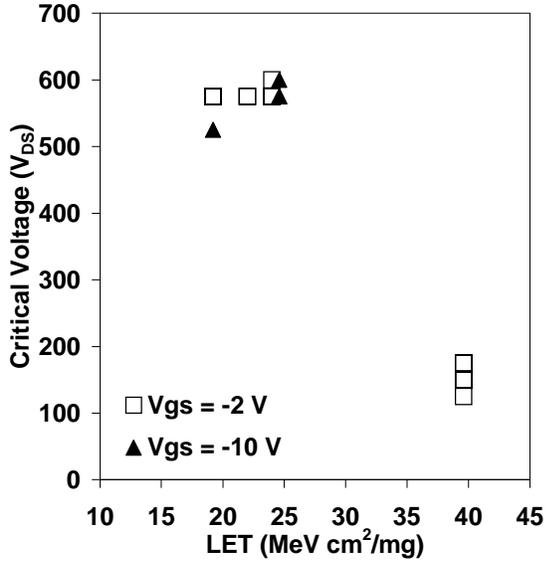Figure 10: Radiation response of APT10088HVR.

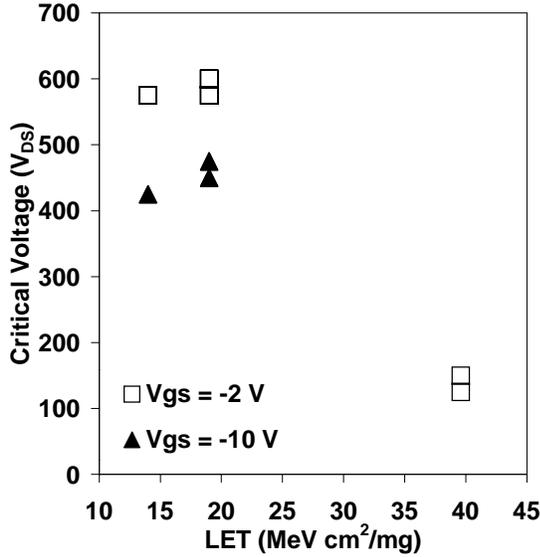Figure 11: Radiation response of the RFP4N100 by Fairchild.

Figure 12: Radiation response of the IRHY7434.

V. ANALYSIS

A. Radiation Environment

In order to calculate SEGR failure rates for the various device types, an orbit of 705km and a 98° inclination was modeled. The orbit-average was a modification of the galactic cosmic ray (GCR). The modified orbit-average made allowance for protection from the earth's magnetic field, optical shadowing by the earth and accounted for the period of solar minimum, see Figure 13. Failure rates during solar maximum (but without solar flares) can be approximated by multiplying the given rates for solar minimum by 1/3 for this orbit. Failure rates for a major solar flare are on the order of the number of SEGRs accumulated from one year of Solar minimum GCR.
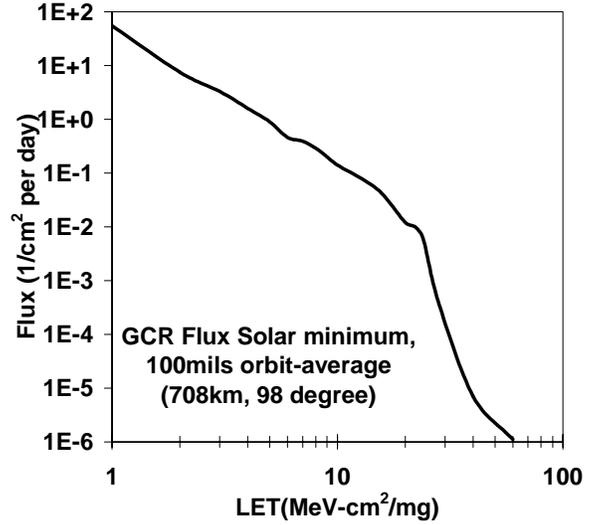

Figure 13:Modeled galactic cosmic ray environment during Solar minimum.

B. "Best Guess" and "Worst Case" criterion:

Currently, there is no accurate method for estimating SEGR failure rates. A reason is that cross section measurements are expensive and time consuming to acquire. In order to generate device cross sections tests of many identical parts would be required. Furthermore, the directional dependence of device susceptibility must be known for accurate rate estimates. Different device families may show different directional effects, so these effects must be measured. This is not possible on a limited budget, so assumptions elaborated below were used. This leads to a "Best Guess" and a "Worst Case" estimate. The "Best Guess" and "Worst Case" rates are tabulated (see Table IV) for each device type using the SEGR onset condition.

1. Worst Case Rate:

i. Normal-Incident Threshold LET:

Because there was no data taken below an LET of 14 MeV-cm²/mg, extrapolating down to lower LETs was difficult. Therefore, an arbitrary assumption was made for the threshold LET. The threshold LET was arbitrarily assigned a value of 5 MeV-cm²/mg. The voltage onset was taken to be equal to the lowest critical voltage for the lowest LET (14 or 19) and bias condition, see Table IV.

ii. Normal-Incident Cross Section:

The observed fluence-to-failure associated with each device type appears to be $\sim 10^{-3}$ cm² based on the in situ measurements (Figures 1 through 4). It is not clear whether the estimate of 10^{-3} cm² is close to the saturation cross section. A conservative assumption is that the cross section

(per device) is the sum of the gate area (which is about 4×10^{-2} cm^2) when the LET is slightly greater than the threshold. However, this is too conservative if the threshold LET is taken to be 5, because the cross section for LET < 14 (or 19) should not exceed the observed cross section at an LET of 14 (or 19). Therefore the device cross section is assumed to be 10^{-3} cm^2 when 5 < LET < 19, and 4×10^{-2} cm^2 when LET > 19.

iii. Directional Effects:

The threshold LET for SEGR typically increases with increasing incident angle. An assumption that is likely quite conservative is that the threshold LET is directional invariant. The directional cross section is assumed to be the projection (in the direction of the particle path) of a flat area in the device plane, which decreases with increasing angle according to a cosine law.

Combining the above assumptions, the SEGR failure rate was calculated from

$$rate = \int_0^\infty h(L)\sigma_{AVE}(L)dL \qquad (1)$$

where h is the differential (in LET) omnidirectional flux, and σ_{AVG} is the directional average cross section. This cross section is given by

$$\sigma_{AVG}(L) = \frac{1}{4\pi}\int_{-1}^{1}\int_0^{2\pi}\sigma(L,\theta,\varphi)d\varphi d(\cos\theta) \qquad (2)$$

where σ is the directional cross section. Assuming azimuthal symmetry, and if there is no distinction between trajectories that are in opposite directions, the equation reduces to

$$\sigma_{AVG}(L) = \int_0^1 \sigma(L,\theta)d(\cos\theta). \qquad (3)$$

The directional cross section is given by

$$\sigma(L,\theta) = \begin{cases} 0 \cdot if \cdot L < 5 \\ 10^{-3}cm^2\cos\theta \cdot if \cdot 5 < L < 19 \\ 4x10^{-2}cm^2\cos\theta \cdot if \cdot L > 19 \end{cases} \qquad (4)$$

substituting equation 4 into 3 yields,

$$\sigma_{AVG}(L) = \begin{cases} 0 \cdot if \cdot L < 5 \\ 5x10^{-4}cm^2 \cdot if \cdot 5 < L < 19 \\ 2x10^{-3}cm^2 \cdot if \cdot L > 19 \end{cases} \qquad (5)$$

Hence, the SEGR failure rate is given by

rate = 5×10^{-4} cm^2 [H(5) – H(19)] + 2×10^{-2} cm^2 H(19)   (6)

where H is the integral omndirectional flux (Figure 13).

2. Best Guess Rate:

i. Normal-Incident Threshold LET:

It was assumed that the threshold LET was not 5 but rather 14 MeV-cm^2/mg.

ii. Normal-Incident Cross Section:

It was assumed that the cross section estimate of 10^{-3} cm^2 applies to large enough LET so that rates can be calculated from a step function having this saturation value.

iii. Directional Effects:

No new assumption where made in this section. Equations (4) and (5) are repeated but with LET of 14 MeV-cm^2/mg is substituted for 5 throughout. Hence, the SEGR failure rate is given by

rate = 5×10^{-4} cm^2 [H(14) – H(19)] + 2×10^{-2} cm^2 H(19)   (7)

The failure rates presented in Table IV, are the for the "Worst Case" and "Best Guess" based on the biasing condition at which the DUT(s) failed.

TABLE IV: "WORST CASE" AND "BEST GUESS" SEGR FAILURE RATES FOR $V_{GS} = -2$ AND -10 VOLTS BIAS CONDITIONS.

Device type	Bias condition at failure					
	Lowest V_{DS} Volts @ V_{GS} = (-2V / -10V)	Avg. V_{DS} volts @ V_{GS} = (-2V / -10V)	LET onset MeV-cm^2/mg		Worst Case	Best Guess
			Worst case assump-tion	Best guess assump-tion	Rate (10^{-4} per day)	Rate (10^{-4} per day)
IRFM G40 (non-flight)	450 450	462.5 450.0	5	14	6.84	2.59
(flight)	450 450	450.0 450.0	5	14	6.84	2.59
IRHY7 G30C MSE	800 850	850.0 862.5	5	14	6.84	2.59
Eng. I	725	725.0	5	14	6.84	2.59
Eng. II	825	900	5	14	6.84	2.59
APT1004RCN	475 475	487.5 487.5	5	14	6.84	2.59
APT10088HVR	450 250	462.5 300.0	5	14	6.84	2.59
RFP4N100	575 425	575 425	5	14	6.84	2.59
IRHY7434	575 575	575 525	5	14	6.84	2.59

VI. Conclusion

A. SEGR failure criterion

The failure criterion for SEGR has been arbitrarily set at 1μA. Figure 3 showed that a gate rupture had taken place during irradiation that drew less than 1μA, which was termed partial SEGR. Perhaps, a modification to the SEGR criterion should be made. The modification ought to consider partial gate ruptures that draw currents that are at least 100 times the pre-irradiation level (and that last several sample periods, i.e., ~1 second or longer) as a failure. By incorporating partial SEGR as failure points, test engineers can provide a better "Best Guess" and "Worst Case" scenario to spacecraft designers. Thus, in-orbit SEGR failure rates can only be estimated in a very crude way.

B. Transient Events

In situ measurements provide an insight to the anatomy of SEGR and SEB failure. Faster sampling rates could improve the present understanding of the mechanism that drive these failure modes. In figure 1 it was observed that the transient currents (source and drain) ultimately led to SEB. The transient currents observed in the gate never increased beyond 2 orders of magnitude, except at the 131st second where the transient current increased by 4 orders of magnitude. These gate current transients did not last longer than the sampling period. The transient currents observed at the gate did not trigger SEB.

Gate rupture was observed to be triggered by transient currents that occurred in the gate (see Figures 2 and 4), which established a current path between gate-to-drain and gate-to-source, respectively. In figure 3, SEGR appears to have been triggered by transient events that originated at the drain and source. Thus, a current path (or paths) was established between gate-to-drain which ultimately led to SEGR. A similar scenario can be inferred to take place for current transients that originate at the source which when couple with current transients at the gate lead to SEGR (a source-to-gate short). This failure mode was not observed within our data set, perhaps this failure mode is very rare.

C. Part-to-Part variability

Some high-voltage power MOSFETS show a large part-to-part variation in critical voltage for a given LET, in particular see Figure 10 (APT10088HVR). However, this variability was observed in most of the radiation response figures.

D. Long-range Ions versus Short-range Ions

Long-range ions (ones that fully penetrate and exit the epitaxial region) were able to cause SEGR at a lower critical voltage than short-range ion as was observed in Figure 7. For that reason, long-range ions are required to characterize SEGR and SEB in high voltage power MOSFETs.

VII. Acknowledgment

VIII. References

[1] T. F. Wrobel, "On Heavy-Ion Induced Hard Errors in Dielectric Structures," IEEE Trans. Nucl. Sci., NS-34, No. 6, pp. 1262-1268, 1987.

[2] C.F. Wheatley, J. L. Titus and D. I. Burton, "Single-Event Gate Rupture in Vertical Power MOSFETs; An Original Empirical Expression," IEEE Trans. Nucl. Sci., NS-41, No. 6, pp. 2152-2159, 1994.

[3] J. H. Hphl and G. H. Johnson, "Features of the Triggering Mechanism for Single Event Burnout in N-Channel Power MOSFETs," IEEE Trans. Nucl. Sci., NS-36, No. 6, pp. 2260-2266, 1989.

[4] G. H. Johnson, R. D. Schrimpf, K. F. Galloway, and R. Koga, "Temperature Dependence of Single-Event Burnout in N-Channel Power MOSFETs," IEEE Trans. Nucl. Sci., NS-39, No. 6, pp. 1605-1612, 1992.

[5] J. L. Titus, C. F. Wheatley, D. I. Burton, I. Mouret, M. Allenspach, J. Brews, R. Schrimpf, K. Galloway, and R. L. Pease, "Impact of Oxide Thickness on SEGR Failure in Vertical Power MOSFETs; Development of a Semi-Empirical Expression," IEEE Trans, Nucl, Sci., NS- 42, No. 6, 1995.

[6] L. E. Selva, G. M. Swift, W. A. Taylor, and L. D. Edmonds, "On The Role of Energy Deposition in Triggering SEGR in Power MOSFETs", IEEE Trans, Nucl, Sci., NS-46, No. 6, 1999.

[7] International Rectifier, Datasheet for IRHY7G30CMSE 1000V, N-Channel Rad Hard HEXFET Technology, PD-93973D, URL: www.irf.com/product-info/datasheets/data/irhy7g30cmse.pdf.